IEEE Access
Multidisciplinary : Rapid Review : Open Access Journal

Received 1 December 2023, accepted 20 January 2024, date of publication 1 February 2024, date of current version 22 February 2024.

Digital Object Identifier 10.1109/ACCESS.2024.3361285

RESEARCH ARTICLE

Fault Diagnosis for Takagi-Sugeno Model Wind Turbine Pitch System

JORGE IVÁN BERMÚDEZ RODRÍGUEZ [1], HÉCTOR RICARDO HERNÁNDEZ-DE-LEÓN [1], (Senior Member, IEEE), JUAN ANZUREZ MARÍN [2], ALEJANDRO MEDINA SANTIAGO [3], ELÍAS NEFTALÍ ESCOBAR GÓMEZ [1], (Member, IEEE), BETTY YOLANDA LÓPEZ ZAPATA [4], AND JULIO ALBERTO GUZMÁN-RABASA [5]

[1]Tecnológico Nacional de México, Campus Tuxtla Gutiérrez, Tuxtla Gutiérrez 29050, Mexico
[2]Facultad de Ingeniería Eléctrica, Universidad Michoacana de San Nicolás de Hidalgo, Morelia 58000, Mexico
[3]Consejo Nacional de Ciencia y Tecnología, Department of Computer Science, Instituto Nacional de Astrofísica, Óptica y Electrónica, Puebla 72840, Mexico
[4]Dirección de Ingeniería Biomédica, Universidad Politécnica de Chiapas, Suchiapa, Chiapas 29150, México
[5]Tecnologico Nacional de México, IT Hermosillo, Hermosillo 83170, Mexico

Corresponding authors: Héctor Ricardo Hernández-de-León (hector.hl@tuxtla.tecnm.mx) and Alejandro Medina Santiago (amedina@inaoep.mx)

ABSTRACT This paper presents a fault diagnosis (FDD) approach based on a Takagi-Sugeno Unknown Input Observer (TS-UIO) that allows for the estimation of the states of an active pitch system for a studied wind turbine even in the presence of unknown interference factors. A scheme for FDD is proposed based on the residual evaluation between the non-linear model of the active pitch system and the Takagi-Sugeno unknown input observer proposed for the detection and isolation of faults in sensors with measurable premise variables. The proposed TS-UIO State Observer is resilient to disturbances and measurement noise due to its unique feature of decoupling unknown inputs, interruptions, or undefined factors that affect the behavior of the system under study. This study investigates the effect of load-induced stress on the mechanical blades of a wind turbine, caused by the wind force considered as an unknown disturbance or input to the system given its dependence on weather conditions. The proposed FDD algorithm includes Linear Matrix Inequalities (LMI) ensuring the estimation error dynamics approximates to zero. Successful implementation tests are demonstrated in an active pitch system with reference parameters based on a wind turbine model. The review outlines traditional FDD approaches, including those based on nonlinear models, as well as relatively new methods based on linear sector conditions. Special attention is given to Takagi-Sugeno (TS) methods.

INDEX TERMS Fault diagnosis, unknown inputs observer, pitch system, Takagi-Sugeno model.

I. INTRODUCTION

The safety and reliability of wind power systems are of utmost importance today due to the increasing demand for electrical energy consumption [1]. Thus, it is necessary to implement monitoring actions to detect faults. In the case of state-of-the-art wind power systems, rapid and efficient fault handling is crucial to anticipate future impacts on the system [2].Therefore, it is necessary to understand the operation of wind turbines, which begins with the conversion of mechanical wind energy into electrical energy through the generator. For this purpose, it is necessary to couple a converter with a rated power equal to the generator's capacity [3]. Next, a gearbox is placed between the rotor and the generator to transmit the rotor's speed to the generator, allowing for speed control [4]. For this reason, the energy generation process can be a complex one that must be controlled by altering the rotor's aerodynamics [5].

The aerodynamics of the rotor can be managed by modifying either the pitch angle of the blades or the rotor speed [6]. The mechanism employed to alter the pitch angle of the blades is referred to as the pitch system. This system is

The associate editor coordinating the review of this manuscript and approving it for publication was Okyay Kaynak.

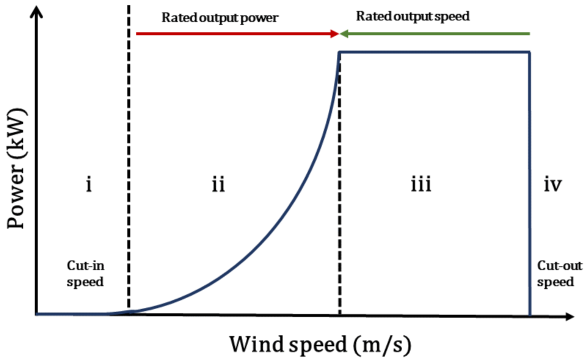

FIGURE 1. The evolution of mechanical power versus wind speed [11].

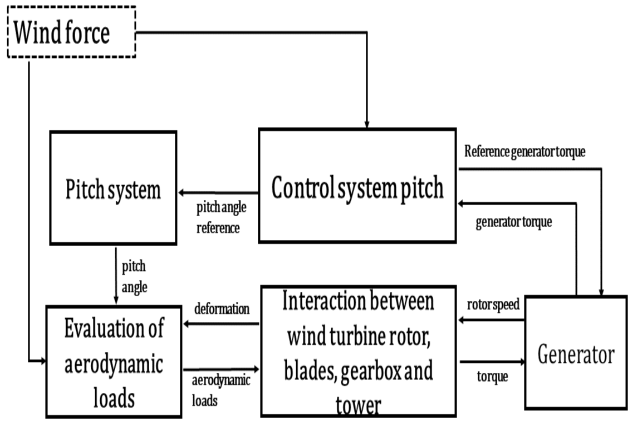

FIGURE 2. Block diagram of active pitch into a wind turbine.

employed to regulate the rotor's speed and the energy output of the wind turbine, ensuring that the wind load on the rotor remains within design limits. By manipulating the pitch angle of the blades, the wind turbine's power coefficient can be maintained or increased, enabling the production of more energy with the same amount of wind. Typically, the pitch system is used in conjunction with other wind turbine control systems to optimize efficiency and energy production [7] can see Figure 2.

When the wind speed is equal to the nominal speed of the wind turbine, a transition occurs between zone 2 and zone 3 of the wind turbine's operation. In zone 2, the wind speed is lower than the nominal speed of the wind turbine, and the kinetic energy of the wind is used to increase the rotor speed of the wind turbine, as observed in Figure 1. In zone 3, the wind speed is higher than the nominal speed of the wind turbine, and the kinetic energy of the wind is used to generate electricity.

For optimal performance, the wind turbine speed must be carefully controlled during the transition from zone 2 to zone 3 to ensure that the maximum amount of energy is produced. The aim of the control is to maintain the output power. This can be achieved by controlling the pitch system, which adjusts the angle of the blades to maintain an optimal rotor speed at different wind speeds. Other control systems, such as generator speed control or tower tilt control, can also be used to optimise wind turbine performance under different wind conditions [2].

A failure must be considered an accidental change in the functionality of the system [8]. Failures of this kind cause an interruption in the standard operation of an automated system, resulting in a decrease in performance that is deemed unacceptable [9]. Thus, it is necessary to study the fault diagnosis and isolation, which are critical to maintaining correct system operation. Allowing enough time to prepare a plan and repair the system [10].

Márquez et al. conducted a literature review in 2012 on the approaches available for monitoring the condition of wind turbines [12]. Gao et al., on the other hand, analysed fault diagnosis and isolation (FDI) approaches based on models and signals, also known as "black box" approaches [13]. While it is true that model-based fault detection and isolation approaches require a complete system model, this can also limit their applicability in some situations. However, in the specific case of wind turbines, these methods can determine the explicit behaviour of the system, making them an advanced monitoring tool. On the other hand, the data-based FDI approach may be affected by the consistency of the recorded data, which reduces its viability. In summary, although data-based approaches are commonly applied to complex processes, model-based approaches tend to have faster response times and can be very useful in monitoring wind turbines.

This work proposes a fault diagnosis (FDI) approach based on signal analysis in the time domain with an explicit mathematical model, mainly in linear models of a wind turbine, obtained from the nonlinear model using the Takagi-Sugeno approach and Unknown Input Observer Takagi-Sugeno (UIO). This new FDI scheme based on UIO represents a valuable reference for fault detection in complex systems, mainly for fault detection and isolation in the pitch system of the wind turbine due to the interaction between the blades attached to the rotor and the gearbox to facilitate the evaluation of aerodynamic loads on the wind turbine rotor, as shown in Figure 2. The proposed method demonstrates high robustness against different stochastic operating conditions and measurement errors at different wind speeds.

This paper is organised as follows: Section II describes the design of the model of an active pitch system [14], Section III describes the pseudocode for Takagi-Sugeno Unknown Input Observer (TS-UIO); Section IV describes the mathematical model of the system under study, which extends to the validated pitch system model; Section V describes the results for Takagi-Sugeno Unknown Input Observer; Section VI describes how to perform a fault detection and isolation (FDI) system in sensors; and Section VII shows simulation results and discussion. Finally, the conclusion is described in Section VIII.

II. STABILITY ANALYSIS AND DESIGN OF A TS-UIO CLASS

Takagi-Sugeno (TS) models are mathematical models that serve as an exact representation of the nonlinear model within a specified range. These models are characterized by their convexity and consist of a set of linear systems interpolated using convex scalar functions, also known as membership or weighting functions, as described in [15]. These functions govern the behavior of the i-th rule and are formulated as follows:

IF α_1(t) is M_{ij} and …and $\alpha_p(t)$ is M_{ip}

$$THEN \begin{cases} \dot{x} = A_i x(t) + B_i u(t) \\ y(t) = C_i x(t) \end{cases} \quad i = 1, 2, \ldots .r \tag{1}$$

where M_{ij} represents a fuzzy set and r denotes the number of rules within the model. The state vector is denoted by $x(t) \in \mathbb{R}^n$, the vector of inputs by $u(t) \in \mathbb{R}^m$, and the vector of outputs by $y(t) \in \mathbb{R}^q$. The terms $A_i \in \mathbb{R}^{n\times n}$ and $C_i \in \mathbb{R}^{q\times n}$ represent coefficient matrices that are associated with each rule. Technical term abbreviations are explained when first utilized. The two known approaches for modeling nonlinear systems are the nonlinear sector method and the linearization method. The former is generally accepted as the more accurate of the two due to its ability to closely represent nonlinear behavior. The latter, as demonstrated in [16], is only an approximate model.

The premise variables can inherently impact the system's rules and are influenced by various factors, including state variables, external disturbances, and time, without relying on any subjective assessments. The measurability of these variables may vary based on the unique characteristics of the case study. It is worth mentioning that selecting a Takagi-Sugeno (TS) system with either measurable or unmeasurable variables depends entirely on the case at hand. The utilization of non-measurable premise variables is closely tied to the particular characteristics of the system being analyzed, the resources available, and the specific goals of the application [17]. In the present study, we have intentionally opted for using TS systems with measurable premise variables. This decision was determined by the feasibility of meeting the instrumentation requirements, as there is no need for estimating non-measurable premise variables. This strategy not only streamlines the system's practical implementation but also lowers the associated expenses.

The vector $\alpha(t)$ groups all individual premise variables, namely $\alpha_1(t)$, and individual premises $\alpha_1(t), \ldots, \alpha_p(t)$. The Takagi-Sugeno model, described in [15], is recommended for consideration.

$$\dot{x}(t) = \sum_{i=1}^{r} h_i(\alpha(t))A_i x(t) + Bu(t) + G\xi(t)$$
$$y(t) = Cx(t) + f_s(t) \tag{2}$$

where $x(t) \in \mathbb{R}^n$ is the state vector, $y(t) \in \mathbb{R}^m$ is the output vector, $u(t) \in \mathbb{R}^r$ is the known input vector, and $\xi(t) \in \mathbb{R}^q$ is the unknown input vector (perturbation), and $f_s(t) \in \mathbb{R}^v$ is the sensor failure vector. B and G, are known matrices with compatible dimensions. A_i represents each of the linear subsystems, and $h_i \in \mathbb{R}$ are weighting functions that depend on $\alpha(t)$, also known as premise variables or determination variables [18]. The weighting functions satisfy the convex sum:

$$\forall i \in [1, 2, \ldots, r], h_1(\alpha(t)) \geq 0,$$
$$\sum_{i=1}^{r} h_i(\alpha(t)) = 1, \forall t \tag{3}$$

There are some papers published in recent years that assume that the premise variables are measurable, as in [19]. However, in some practical applications, the premise variables are not measurable or are measured with level uncertainties [20].

A. UNKNOWN INPUT OBSERVER DESIGN

Unlike conventional unknown input observers, which have been shown to work well in systems with accurate and well-defined models, Takagi-Sugeno unknown input observers (TS-UIO) provide a flexible and adaptable solution for addressing more complex behaviors in systems with inherent uncertainty, high nonlinearity, and imprecision typical of fuzzy systems [21].

In this paper, we present a comprehensive investigation into the application of fuzzy unknown input observers. Through a detailed analysis of the advantages and real-world applications, we demonstrate the value of this approach in improving system performance and efficiency. Our findings illustrate the fundamental importance of this concept in accurately estimating nonlinear and complex systems, thus highlighting its relevance within various engineering and control disciplines. The study builds on prior research that demonstrated the efficacy and utility of Takagi-Sugeno fuzzy observers in approximating nonlinear systems. Specifically, this study focuses on utilizing the fuzzy observer approach for detecting sensor faults in a wind turbine's pitch system with unknown inputs. This perspective adds to the expanding knowledge base in the field of sensor fault detection, endorsing the enduring value of Takagi-Sugeno models in resolving intricate and pertinent issues [22].

In model-based fault diagnosis methods, one topic of great interest is robust residual generation based on fault decoupling approaches [23]. Here, an unknown input is assumed in the system, which is described by a known distribution matrix. This enables the decoupling of the unknown input from the residuals. For an observer with unknown input for a linear system, the estimation error approaches zero even in the presence of the unknown input, since the residual is also decoupled [8].

The structure of a complete order observer is described by:

$$\dot{z}(t) = \sum_{i=1}^{r} h_i(\alpha(t))\Big(F_i z(t) + T_i Bu(t) + K_i y(t)\Big)$$

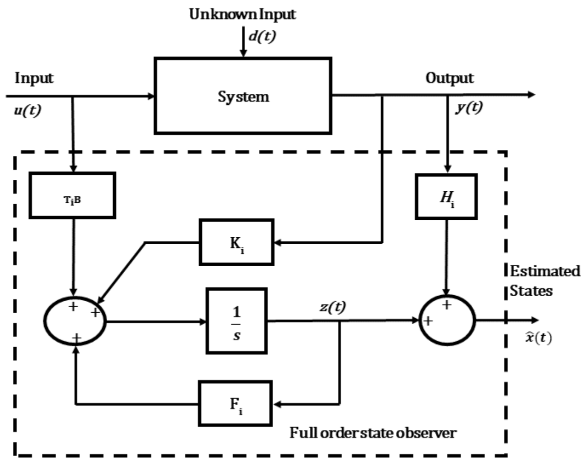

FIGURE 3. Unknown Input Observer Structure [8].

$$\hat{x}(t) = \sum_{i=1}^{r} h_i(\alpha(t)) H_i y(t) + z(t) \tag{4}$$

where $\hat{x} \in \mathbb{R}^2$ is the estimated state vector, $z \in \mathbb{R}^2$ is the observer complete order state vector, and F_i, T_i, K_i, H_i are matrices used to satisfy decoupling of unknown entries and other design requirements [24]. The observer described by equation (4) is shown in Figure 3.

When the observer of the equation (4) is applied to the system 2, the estimated error state is [25]:

$$e(t) = x(t) - \hat{x}(t) \tag{5}$$

The estimate of the error is given by the equation (5), and $\hat{x}(t)$ is then described in equation (4):

$$e(t) = x(t) - \sum_{i=1}^{r} h_i(\alpha(t)) H_i y(t) - z(t) \tag{6}$$

Substituting $y(t) = Cx(t) + f_S(t)$

$$e(t) = x(t) - \sum_{i=1}^{r} h_i\big(\alpha(t)\big) H_i \,\big(Cx(t) + f_S(t)\,\big) - z(t) \tag{7}$$

To obtain the dynamics of the error, equation (5) is derived by substituting $\dot{z}(t)$ from equation (4) [26], which is described in the following equation:

$$\begin{aligned}
\dot{e}(t) &= \sum_{i=1}^{r} h_i\big(\alpha(t)\big)\,[I - H_i C]\,\dot{x}(t) \\
&\quad - \sum_{i=1}^{r} h_i\big(\alpha(t)\big) H_i \dot{f}_s(t) - \dot{z}(t) \\
\dot{e}(t) &= \sum_{i=1}^{r} h_i\big(\alpha(t)\big)\,[I - H_i C] \\
&\quad \times \left(\sum_{j=1}^{r} h_j\big(\alpha(t)\big) A_j x(t) + Bu(t) + G\xi(t) \right) \\
&\quad - \sum_{i=1}^{r} h_i\big(\alpha(t)\big) H_i \dot{f}_s \\
&\quad - \sum_{i=1}^{r} h_i\big(\alpha(t)\big) \Big(F_i z(t) + T_i Bu(t) + K_i Cx(t) \Big)
\end{aligned} \tag{8}$$

grouping terms:

$$\begin{aligned}
\dot{e}(t) &= \sum_{i=1}^{r} h_i(\alpha(t)) \Bigg(\sum_{j=1}^{r} h_j(\alpha(t)) A_j x(t) + Bu(t) + G\xi(t) \\
&\quad - \sum_{j=1}^{r} h_j(\alpha(t)) H_i C A_j x(t) - H_i C B u(t) \\
&\quad - H_i C G \xi(t) \Bigg) - \sum_{i=1}^{r} h_i\big(\alpha(t)\big) H_i \dot{f}_s(t) \\
&\quad - \sum_{i=1}^{r} h_i\big(\alpha(t)\big) \Big(F_i z(t) + T_i Bu(t) + K_i y(t) \Big)
\end{aligned} \tag{9}$$

substituting $y(t) = Cx(t) + f_S(t)$:

$$\begin{aligned}
\dot{e}(t) &= \sum_{i=1}^{r} h_i(\alpha(t)) \Bigg(\sum_{j=1}^{r} h_j(\alpha(t)) A_j x(t) + Bu(t) + G\xi(t) \\
&\quad - \sum_{j=1}^{r} h_j(\alpha(t)) H_i C A_j x(t) - H_i C B u(t) \\
&\quad - H_i C G \xi(t) \Bigg) - \sum_{i=1}^{r} h_i\big(\alpha(t)\big) H_i \dot{f}_s(t) - \sum_{i=1}^{r} h_i\big(\alpha(t)\big) \\
&\quad \times \Big(F_i z(t) + T_i Bu(t) + K_i Cx(t) + K_i f_s(t) \Big)
\end{aligned}$$

grouping terms:

$$\begin{aligned}
\dot{e}(t) &= \sum_{i=1}^{r} \sum_{j=1}^{r} h_i(\alpha(t)) h_j(\alpha(t)) A_j x(t) \\
&\quad - \sum_{i=1}^{r} \sum_{j=1}^{r} h_i(\alpha(t)) h_j(\alpha(t)) H_i C A_j x(t) \\
&\quad - \sum_{i=1}^{r} h_i(\alpha(t)) K_i C x(t) \\
&\quad + \sum_{i=1}^{r} h_i(\alpha(t)) B u(t) - \sum_{i=1}^{r} h_i(\alpha(t)) H_i C B u(t) \\
&\quad - \sum_{i=1}^{r} h_i(\alpha(t)) T_i B u(t) + \sum_{i=1}^{r} h_i(\alpha(t)) G \xi(t) \\
&\quad - \sum_{i=1}^{r} h_i(\alpha(t)) H_i C G \xi(t) - \sum_{i=1}^{r} h_i(\alpha(t)) H_i \dot{f}_s(t) \\
&\quad - \sum_{i=1}^{r} h_i(\alpha(t)) K_i f_s(t) - \sum_{i=1}^{r} h_i(\alpha(t)) F_i z(t)
\end{aligned} \tag{10}$$

Solving for $z(t)$ in (7) and substituting into (10) the dynamics of error can be expressed as:

$$\dot{e}(t) = \sum_{i=1}^{r}\sum_{j=1}^{r} h_i(\alpha(t))h_j(\alpha(t))\big(A_j - H_iCA_j - K_iC\big)x(t) + \sum_{i=1}^{r} h_i(\alpha(t))(B - H_iCB - T_iB)u(t) - \sum_{i=1}^{r} h_i(\alpha(t))(G - H_iCG)\xi(t) - \sum_{i=1}^{r} h_i(\alpha(t))H_i\dot{f}_s(t) - \sum_{i=1}^{r} h_i(\alpha(t))K_if_s(t) - \sum_{i=1}^{r} h_i(\alpha(t))Fi \times \left(\sum_{i=1}^{r} h_i(\alpha(t))(I - H_iC)x(t) - e(t)\right) \quad (11)$$

finally, the dynamics of the error can be expressed as:

$$\dot{e}(t) = \sum_{i=1}^{r}\sum_{j=1}^{r} h_i(\alpha(t))h_j(\alpha(t))\Big(A_j - H_iCA_j - K_iC + F_iH_iC - F_i\Big)x(t) + \sum_{i=1}^{r} h_i(\alpha(t))\Big(B - H_iCB - T_iB\Big)u(t) - \sum_{i=1}^{r} h_i(\alpha(t))(G - H_iCG)\xi(t) - \sum_{i=1}^{r} h_i(\alpha(t))H_i\dot{f}_s(t) - \sum_{i=1}^{r} h_i(\alpha(t))K_if_s(t) + \sum_{i=1}^{r} h_i(\alpha(t))F_ie(t) \quad (12)$$

Remark 1: In order for the observer to prove its efficiency, the error $e(t)$ should asymptotically approach zero, which means that the estimated state $\hat{x}(t)$ should approach the actual state of the system $x(t)$ in the absence of faults, where $f_s(t) = 0$ and $\dot{f}_s(t) = 0$. The following relationships must hold true to achieve this goal:

$$\sum_{i=1}^{r} h_i(\alpha(t))(B - H_iCB - T_iB)u(t) = 0$$
$$T_i = I - H_iC \quad (13)$$
$$\sum_{i=1}^{r} h_i(\alpha(t))(G - H_iCG)\xi(t) = 0$$
$$G = H_iCG \quad (14)$$

Considering the relationships (13) and (14), we obtain

$$\sum_{i=1}^{r}\sum_{j=1}^{r} h_i(\alpha(t))h_j(\alpha(t))(I - H_iC)A_j = \sum_{j=1}^{r}\sum_{i=1}^{r} h_i(\alpha(t))h_j(\alpha(t))T_iA_j \quad (15)$$

Remark 2: The following variable changes (16, 17,18) are proposed to simplify the term that multiplies $x(t)$ in the equation (12).

$$\sum_{i=1}^{r}\sum_{j=1}^{r} h_i(\alpha(t))h_j(\alpha(t))T_iA_j = \sum_{i=1}^{r} h_i(\alpha(t))A1_i \quad (16)$$
$$\sum_{i=1}^{r} h_i(\alpha(t))F_iH_i = \sum_{i=1}^{r} h_i(\alpha(t))K2_i \quad (17)$$
$$\sum_{i=1}^{r} h_i(\alpha(t))K_i = \sum_{i=1}^{r} h_i(\alpha(t))(K1_i + K2_i) \quad (18)$$

Such that the dynamics of the error can be rewritten as:

$$\dot{e}(t) = \sum_{i=1}^{r} h_i(\alpha(t))\Big(A1_i - K_iC + K2_iC - F_i\Big)x(t) + \sum_{i=1}^{r} h_i(\alpha(t))F_ie(t) \quad (19)$$

therefore:

$$\sum_{i=1}^{r} h_i(\alpha(t))\Big(A1_i - K_iC + K2_iC - F_i\Big)x(t) = 0$$
$$F_i = A1_i - K_iC + K2_iC \quad (20)$$

Theorem 1: For the TS system (2), an asymptotic Unknown Input Observer (UIO) (4) is proposed with gains K_i, H_i, T_i and F_i that satisfy conditions (13) and (14) if and only if there exists a positive definite matrix $P = P^T \in \mathbb{R}^{mxm}$ and $\chi \in \mathbb{R}^{mxm}$ that satisfies the LMIs:

$$P > 0$$
$$A1_i^TP - \chi_i^TC^T + PA1_i - \chi_iC < 0 \quad (21)$$

Proof: Given the conditions from 20, the dynamics of the error are expressed as:

$$\dot{e}(t) = \sum_{i=1}^{r} h_i(\alpha(t))F_ie(t) \quad (22)$$

Considering a candidate Lyapunov function as a function of the error:

$$v(e(t)) = e(t)^TPe(t) > 0 \quad (23)$$

where:

$$P = P^T > 0$$

Therefore, the derivative of the function is monotonically decreasing, as can be seen:

$$\dot{v}\big(e(t)\big) < 0 \quad (24)$$
$$\dot{v}\big(e(t)\big) = \dot{e}(t)^TPe(t) + e(t)^TP\dot{e}(t) < 0 \quad (25)$$

Given the fact that the sum of $\sum_{i=1}^{r} h_i(\alpha(t)) = 1$ and the weights are between zero and one and substituting (22) in (25):

$$\left(F_i e(t)\right)^T Pe(t) + e(t)^T P\left(F_i e(t)\right) < 0 \tag{26}$$

We have that the LMIs $F_i^T P + PF_i < 0, i = 1, 2, \ldots, r$ are sufficient conditions for $\dot{v}\left(e(t)\right) < 0$.

$$\left(A1_i - K1_i C\right)^T P + P\left(A1_i - K1_i C\right) < 0 \tag{27}$$

A change of variable is proposed for:

$$\chi_i = PK1_i \Rightarrow K1_i = P^{-1}\chi_i$$
$$\chi_i^T = K1_i^T P$$

Finally, the LMI can be expressed as follows:

$$A1_i^T P - \chi_i^T C^T + PA1_i - \chi_i C < 0 \tag{28}$$

This concludes the proof □

III. PSEUDOCODE FOR OBSERVER DESIGN

This section is dedicated to presenting the procedure for designing the unknown input observer.

- Step 1: Calculate T_i and H_i and $A1$

$$\left[T_i H_i\right] = \left(\begin{bmatrix} I \\ C \end{bmatrix}^T \begin{bmatrix} I \\ C \end{bmatrix}\right)^{-1} \begin{bmatrix} I \\ C \end{bmatrix}^T$$
$$A1_i = T_i A_j$$

- Step 2: LMI solution from 28
- Step 3: Calculate F_i

$$F_i = A1_i - K1_i C$$

- Step 4: Calculate K

$$K2_i = F_i H_i$$
$$K_i = K1_i + K2_i$$

IV. MODELING OF AN ACTIVE PITCH SYSTEM

In this section, the parts of the pitch system model are presented. Finally, the numerical values of the various parameters are given.

A. PITCH SYSTEM MODEL

The pitch system consists of four main components [4]:

- Gear train consisting of a frequency converter, an electric motor (a squirrel cage rotor), a gearbox, and a transmission pinion.
- Rotor Blade Rotary Union
- Wind rotor blade
- Gearbox control unit. The gearbox control unit receives the desired angle of attack φ from the control system and calculates the control signal for the motor. The power of the motor is converted into speed and torque by the gearbox.

Similarly, the vectors, whose components are the stator and rotor currents, For an induction motor with one pair of poles, the equations describing the induction motor are thus:

$$\begin{aligned}
\dot{x_1}(t) &= -\frac{R_s}{\sigma L_s}\left(x_1(t) - \frac{L_m}{L_r}x_3(t)\right) + \omega_s x_2(t) + u_1(t) \\
\dot{x_2}(t) &= -\frac{R_s}{\sigma L_s}\left(X_2(t) - \frac{L_m}{L_r}x_4(t)\right) - \omega_s x_1(t) + u_2(t) \\
\dot{x_3}(t) &= -\frac{R_r}{\sigma L_r}\left(x_3(t) - \frac{L_m}{L_s}x_1(t)\right) + \left(\omega_s - px_5(t)\right)x_4(t) \\
\dot{x_4}(t) &= -\frac{R_r}{\sigma L_r}\left(x_4(t) - \frac{L_m}{L_s}x_2(t)\right) - \left(\omega_s - px_5(t)\right)x_3(t) \\
\dot{x_5}(t) &= \frac{3}{2}\frac{Z_p}{J}\frac{L_m}{\sigma L_s L_r}\left(x_2(t)x_3(t) - x_1(t)x_4(t)\right) - \frac{T_L}{i_g J} \\
\dot{x_6}(t) &= x_5(t)
\end{aligned} \tag{29}$$

The state variables are:

$$\begin{aligned}
x(t) &= [x_1(t)\ x_2(t)\ x_3(t)\ x_4(t)\ x_5(t)\ x_6(t)]^T \\
&:= [\psi_{sd}(t)\ \psi_{sq}(t)\ \psi_{rd}(t)\ \psi_{rq}(t)\ \omega_r(t)\ \varphi(t)]^T
\end{aligned}$$

and

$$u(t) = [u_1(t)\ u_2(t)]^T := [u_{sd}(t)\ u_{sq}(t)]^T \tag{30}$$

The state variables $\psi_{sd}(t)$ and $\psi_{sq}(t)$ are the components of the magnetic flux in the stator within the frames d and q, $\psi_{rd}(t)$ and $\psi_{rq}(t)$ are the components of the magnetic flux in the rotor within the frames d and q, $\omega_r(t)$ is the rotor speed, and $\varphi(t)$ is the rotor angle. The input vector contains the stator voltages $u_{sd}(t)$, $u_{sq}(t)$ are also related in the frames d and q. The system parameters in equation (29) are the load inertia J, the stator and rotor resistance R_s and R_r, the stator and rotor inductance L_s and L_r, the mutual inductance L_m, the number of pole pairs p and $\sigma = L_s - \frac{L_m^2}{L_s L_r}$ is the Blondel coefficient, and the relationship $\gamma = \frac{3}{2}\frac{p}{J}\frac{L_m}{\sigma L_s L_r}$ is used to simplify the writing of the equation(33). The transmission ratio that exists between the gearbox and the spur gears connecting the wind turbine blades $i_g = i_{gp}\ i_{gs}$. The total moment of inertia is the sum of the moment of inertia of the induction motor J_a, the moment of inertia of the gear Jg, and the moment of inertia about the axial length of the blade Jg.

$$J = J_a + J_g + \frac{J_b}{i_g^2} \tag{31}$$

The system output vector is defined as: $y(t) := [i_{sq}(t), i_{sd}(t), \omega_b(t), \varphi(t)]$ from state space model equation (32).

$$y(t) = \begin{bmatrix} \frac{1}{\sigma L_s} & 0 & -\frac{L_m}{\sigma L_s L_r} & 0 & 0 & 0 \\ 0 & \frac{1}{\sigma L_s} & 0 & -\frac{L_m}{\sigma LsL_r} & 0 & 0 \\ 0 & 0 & 0 & 0 & \frac{1}{i_g} & 0 \\ 0 & 0 & 0 & 0 & 0 & \frac{1}{i_g} \end{bmatrix} \times [\psi_{sd}(t)\ \psi_{sq}(t)\ \psi_{rd}(t)\ \psi_{rq}(t)\ \omega_r(t)\ \varphi(t)]^T \tag{32}$$

TABLE 1. pitch system parameters.

R_s	L_s	J_g	L_r	p
0.8817Ω	$0.1094H$	$0.2Kgm^2$	$0.1071H$	3
L_m	J_b	R_r	J_a	i_g
$0.1054H$	$1977\ Kgm^2$	0.4321Ω	$0.4724\ Kgm^2$	1200

The parameters of the pitch system described by equation(29) are shown in Table 1.

The approach used in the present research, "non-linear sector", is explained in [16]. This approach guarantees the accurate construction of fuzzy models. The pitch system (see equation (29)) is considered a simple nonlinear system $\dot{x}$(t)= f(x(t)) where $f(0) = 0$. The objective is to find the local sector such that $\dot{x}$(t)= f(x(t)) $\in [a_1 a_2]$. Such local sectors whose nonlinearities are denoted by $x_3(t) \in [-0.4, 0.4]$ (Wb), $x_4(t) \in [-0.4, 0.4]$ (Wb) and $w(t) \in [-378, 378]$ rad/s.

The assumption variables $\alpha_1(t) = \omega(t)$, $\alpha_2(t) = x_4(t)$, $\alpha_3(t) = x_3(t)$ are used to compute the membership functions, and the resulting TS model is:

$$A_i = \begin{bmatrix} -\frac{R_s}{\sigma L_s} & \alpha_1(i) & -\frac{L_m R_s}{\sigma L_s L_r} & 0 & 0 & 0 \\ -\alpha_1(i) & -\frac{R_s}{\sigma L_s} & 0 & -\frac{R_s L_m}{\sigma L_s L_r} & 0 & 0 \\ \frac{R_r L_r}{\sigma L_s L_r} & 0 & -\frac{R_r}{\sigma L_r} & \alpha_1(i) & -p\alpha_2(i) & 0 \\ 0 & \frac{R_r L_n}{\sigma L_s L_r} & -\alpha_1(i) & -\frac{R_r}{\sigma L_r} & p\alpha_3(i) & 0 \\ -\gamma\alpha_2(i) & \gamma\alpha_3(i) & 0 & 0 & 0 & 0 \\ 0 & 0 & 0 & 0 & 1 & 0 \end{bmatrix} \tag{33}$$

$$B = \begin{bmatrix} 1 & 0 \\ 0 & 1 \\ 0 & 0 \\ 0 & 0 \\ 0 & 0 \\ 0 & 0 \end{bmatrix} \quad G = \begin{bmatrix} 0 & 0 & 0 & 0 & -\frac{1}{igJ} & 0 \end{bmatrix}^T \tag{34}$$

The matrix C is defined by:

$$C = \begin{bmatrix} \frac{1}{\sigma L_s} & 0 & -\frac{L_m}{\sigma L_s L_r} & 0 & 0 & 0 \\ 0 & \frac{1}{\sigma L_s} & 0 & -\frac{L_m}{\sigma L_s L_r} & 0 & 0 \\ 0 & 0 & 0 & 0 & \frac{1}{ig} & 0 \\ 0 & 0 & 0 & 0 & 0 & \frac{1}{ig} \end{bmatrix} \tag{35}$$

Membership functions are:

$$M_1(\alpha_1(t)) = \frac{\alpha_1(t)+378}{756}\ ;\ M_2(\alpha_1(t)) = \frac{378-\alpha 1(t)}{756} \tag{36}$$

$$N_1(\alpha_2(t)) = \frac{\alpha_2(t)+0.4}{0.8}\ ;\ N_2(\alpha_2(t)) = \frac{0.4-\alpha_2(t)}{0.8} \tag{37}$$

$$S_1(\alpha_3(t)) = \frac{\alpha_3(t)+0.4}{0.8}\ ;\ S_2(\alpha_3(t)) = \frac{0.4-\alpha_3(t)}{0.8} \tag{38}$$

The weights of which are:

$$\begin{aligned} h_1(\alpha(t)) &= M_1(\alpha_1(t))N_1(\alpha_2(t))S_1(\alpha_3(t) \\ h_2(\alpha(t)) &= M_1(\alpha_1(t))N_1(\alpha_2(t))S_2(\alpha_3(t)) \\ h_3(\alpha(t)) &= M_1(\alpha_1(t))N_2(\alpha_2(t))S_1(\alpha_3(t)) \\ h_4(\alpha(t)) &= M_1(\alpha_1(t))N_2(\alpha_2(t))S_2(\alpha_3(t)) \\ h_5(\alpha(t)) &= M_2(\alpha_1(t))N_1(\alpha_2(t))S_1(\alpha_3(t)) \\ h_6(\alpha(t)) &= M_2(\alpha_1(t))N_1(\alpha_2(t))S_2(\alpha_3(t)) \\ h_7(\alpha(t)) &= M_2(\alpha_1(t))N_2(\alpha_2(t))S_1(\alpha_3(t)) \\ h_8(\alpha(t)) &= M_2(\alpha_1(t))N_2(\alpha_2(t))S_2(\alpha_3(t)) \end{aligned} \tag{39}$$

The matrices A_i obtained are:

$$A_1 = 1 \times 10^3 \times \begin{bmatrix} -1.4207 & 0.3780 & 1.3981 & 0 & 0 & 0 \\ -0.3780 & -1.4207 & 0 & 1.3981 & 0 & 0 \\ 0.6852 & 0 & -0.7112 & 0.3780 & -0.0012 & 0 \\ 0 & 0.6852 & -0.3780 & -0.7112 & 0.0012 & 0 \\ -4.2362 & 4.2362 & 0 & 0 & 0 & 0 \\ 0 & 0 & 0 & 0 & 0.0010 & 0 \end{bmatrix}$$

$$A_2 = 1 \times 10^3 \times \begin{bmatrix} -1.4207 & 0.3780 & 1.3981 & 0 & 0 & 0 \\ -0.3780 & -1.4207 & 0 & 1.3981 & 0 & 0 \\ 0.6852 & 0 & -0.7112 & 0.3780 & -0.0012 & 0 \\ 0 & 0.6852 & -0.3780 & -0.7112 & -0.0012 & 0 \\ -4.2362 & -4.2362 & 0 & 0 & 0 & 0 \\ 0 & 0 & 0 & 0 & 0.0010 & 0 \end{bmatrix}$$

$$A_3 = 1 \times 10^3 \times \begin{bmatrix} -1.4207 & 0.3780 & 1.3981 & 0 & 0 & 0 \\ -0.3780 & -1.4207 & 0 & 1.3981 & 0 & 0 \\ 0.6852 & 0 & -0.7112 & 0.3780 & 0.0012 & 0 \\ 0 & 0.6852 & -0.3780 & -0.7112 & 0.0012 & 0 \\ 4.2362 & 4.2362 & 0 & 0 & 0 & 0 \\ 0 & 0 & 0 & 0 & 0.0010 & 0 \end{bmatrix}$$

$$A_4 = 1 \times 10^3 \times \begin{bmatrix} -1.4207 & 0.3780 & 1.3981 & 0 & 0 & 0 \\ -0.3780 & -1.4207 & 0 & 1.3981 & 0 & 0 \\ 0.6852 & 0 & -0.7112 & 0.3780 & 0.0012 & 0 \\ 0 & 0.6852 & -0.3780 & -0.7112 & -0.0012 & 0 \\ 4.2362 & -4.2362 & 0 & 0 & 0 & 0 \\ 0 & 0 & 0 & 0 & 0.0010 & 0 \end{bmatrix}$$

$$A_5 = 1 \times 10^3 \times \begin{bmatrix} -1.4207 & -0.3780 & 1.3981 & 0 & 0 & 0 \\ 0.3780 & -1.4207 & 0 & 1.3981 & 0 & 0 \\ 0.6852 & 0 & -0.7112 & -0.3780 & -0.0012 & 0 \\ 0 & 0.6852 & 0.3780 & -0.7112 & 0.0012 & 0 \\ -4.2362 & 4.2362 & 0 & 0 & 0 & 0 \\ 0 & 0 & 0 & 0 & 0.0010 & 0 \end{bmatrix}$$

$$A_6 = 1 \times 10^3 \times \begin{bmatrix} -1.4207 & -0.3780 & 1.3981 & 0 & 0 & 0 \\ 0.3780 & -1.4207 & 0 & 1.3981 & 0 & 0 \\ 0.6852 & 0 & -0.7112 & -0.3780 & -0.0012 & 0 \\ 0 & 0.6852 & 0.3780 & -0.7112 & -0.0012 & 0 \\ -4.2362 & -4.2362 & 0 & 0 & 0 & 0 \\ 0 & 0 & 0 & 0 & 0.0010 & 0 \end{bmatrix}$$

$$A_7 = 1 \times 10^3 \times \begin{bmatrix} -1.4207 & -0.3780 & 1.3981 & 0 & 0 & 0 \\ 0.3780 & -1.4207 & 0 & 1.3981 & 0 & 0 \\ 0.6852 & 0 & -0.7112 & -0.3780 & 0.0012 & 0 \\ 0 & 0.6852 & 0.3780 & -0.7112 & 0.0012 & 0 \\ 4.2362 & 4.2362 & 0 & 0 & 0 & 0 \\ 0 & 0 & 0 & 0 & 0.0010 & 0 \end{bmatrix}$$

$$A_8 = 1 \times 10^3 \times \begin{bmatrix} -1.4207 & -0.3780 & 1.3981 & 0 & 0 & 0 \\ 0.3780 & -1.4207 & 0 & 1.3981 & 0 & 0 \\ 0.6852 & 0 & -0.7112 & -0.3780 & 0.0012 & 0 \\ 0 & 0.6852 & 0.3780 & -0.7112 & -0.0012 & 0 \\ 4.2362 & -4.2362 & 0 & 0 & 0 & 0 \\ 0 & 0 & 0 & 0 & 0.0010 & 0 \end{bmatrix}$$

To check the effectiveness of the proposed model, the mean squared error (MSE) is calculated using the equation:

$$MSE = \frac{1}{n}\sum_{i=1}^{n}(P_i - O_i)^2 \tag{40}$$

where:

P_i = Values obtained from the non-linear model

O_i = Values obtained from the TS model

n = Number of sample data

The result obtained is $MSE_1 = 4 \times 10^{-5}$ and $MSE_2 = 5 \times 10^-5$ where MSE_1 is the mean square error between I_{sd} representing the output current in the stator of the stepper actuator at coordinate d of the non-linear model and $I_{sd}TS$ representing the output current in the stator of the stepper actuator at coordinate d of the Takagi-Sugeno model, and MSE_2 is the mean square error between I_{sq} representing the output current in the stator of the stepping actuator at coordinate q of the non-linear model and $I_{sq}TS$ representing the output current in the stator of the stepping actuator at coordinate q of the Takagi-Sugeno model. Therefore, we can check the efficiency of both models in figure 4.

V. RESULTS

In nonlinear system estimation, observers of unknown inputs are crucial. However, the presence of unknown inputs can introduce complexities to the estimation process. To improve estimation performance, we address the challenge of decoupling unknown inputs and enhancing system estimation accuracy.

The primary method for decoupling incorporates the use of filtering methods to separate unknown inputs. Our proposed approach involves employing adaptive filtering techniques or modal decomposition to efficiently extract the influences of unknown inputs from the estimation process.

Our findings demonstrate that the implementation of the proposed decoupling technique effectively enhances the observer's capacity to precisely approximate the system state, despite the presence of unknown inputs. Such an improvement is of paramount importance in various pertinent applications, including the control of dynamic systems and navigation systems, where the accuracy of state estimation is indispensable.

This work contributes to the field by providing a robust methodology for decoupling unknown inputs in observers of nonlinear systems, thus extending the applicability and effectiveness of these observers in real-world environments.

Traditional TS observers operate under global sector conditions where the membership function is limited by constraints on input variables to ensure system stability. However, our proposed new approach is innovative as it adopts a local sector framework, thereby guaranteeing convexity intrinsically through a lack of overlap between the input variables' membership functions. This approach, presented below, offers a promising perspective for improving the efficiency and stability of TS observers, providing a valuable alternative in the design of dynamic systems.

The pitch system (see equation 29) is considered a simple non-linear system $\dot{x}(t) = f(x(t))$ where $f(0) = 0$. The objective is to find the local sector such that $\dot{x}(t) = f(x(t)) \in [a_1 a_2]$. The nonlinearities of the local sectors are denoted by $x_3(t) \in [-0.4, 0.4](Wb)$, $x_4(t) \in [-0.4, 0.4](Wb)$ y $w(t) \in [-378, 378]\ rad/s$.

$$P = \begin{bmatrix} 0.6723 & 0.1339 & -0.3297 & 0.1891 & -0.0278 & 0.0496 \\ 0.1339 & 0.1387 & 0.1375 & 0.1981 & -0.0262 & 0.0467 \\ -0.3297 & 0.1375 & 0.6651 & 0.1941 & -0.0285 & 0.0509 \\ 0.1891 & 0.1981 & 0.1941 & 0.2877 & -0.0364 & 0.0650 \\ -0.0278 & -0.0262 & -0.0285 & -0.0364 & 0.0054 & -0.0096 \\ 0.0496 & 0.0467 & 0.0509 & 0.0650 & -0.0096 & 0.0172 \end{bmatrix} \tag{41}$$

$$F_1 = 1 \times 10^3 \times \begin{bmatrix} 0.0997 & 0.8702 & -0.1165 & -0.4844 & -0.0006 & 0.0000 \\ 0.0164 & -0.1821 & -0.3881 & 0.1608 & 0.0006 & 0.0000 \\ 0.1018 & 0.5099 & -0.1189 & -0.1238 & -0.0006 & 0.0000 \\ 0.2711 & -0.1656 & -0.6448 & 0.1443 & 0.0006 & 0.0000 \\ 0.8663 & 8.8729 & -5.0215 & -4.5631 & -0.0020 & -0.0018 \\ -3.3844 & 0.9662 & 3.3307 & -0.9508 & -0.0001 & -0.0024 \end{bmatrix}$$

$$F_2 = 1 \times 10^3 \times \begin{bmatrix} 0.0756 & 0.0827 & -0.0929 & 0.2906 & -0.0006 & 0.0001 \\ 0.0541 & -0.0572 & -0.4253 & 0.0378 & -0.0006 & -0.0001 \\ 0.1120 & 0.2132 & -0.1289 & 0.1682 & -0.0006 & 0.0000 \\ -0.1330 & -0.0837 & -0.2471 & 0.0637 & -0.0006 & 0.0000 \\ 0.4552 & -0.1271 & -4.6169 & -4.0438 & 0.0000 & -0.0048 \\ 2.2777 & 2.0084 & -2.2416 & -1.9765 & 0.0010 & -0.0044 \end{bmatrix}$$

$$F_3 = 1 \times 10^3 \times \begin{bmatrix} 0.0756 & 0.0827 & -0.0929 & 0.2906 & 0.0006 & -0.0001 \\ 0.0541 & -0.0572 & -0.4253 & 0.0378 & 0.0006 & 0.0001 \\ 0.1120 & 0.2132 & -0.1289 & 0.1682 & 0.0006 & -0.0000 \\ -0.1330 & -0.0837 & -0.2471 & 0.0637 & 0.0006 & 0.0000 \\ -0.4552 & 0.1271 & 4.6169 & 4.0438 & -0.0000 & -0.0048 \\ -2.2777 & -2.0084 & 2.2416 & 1.9765 & 0.0010 & -0.0044 \end{bmatrix}$$

$$F_4 = 1 \times 10^3 \times \begin{bmatrix} 0.0997 & 0.8702 & -0.1165 & -0.4844 & 0.0006 & 0.0000 \\ 0.0164 & -0.1821 & -0.3881 & 0.1608 & -0.0006 & 0.0000 \\ 0.1018 & 0.5099 & -0.1189 & -0.1238 & 0.0006 & 0.0000 \\ 0.2711 & -0.1656 & -0.6448 & 0.1443 & -0.0006 & 0.0000 \\ -0.8663 & -8.8729 & 5.0215 & 4.5631 & -0.0020 & -0.0018 \\ 3.3844 & -0.9662 & -3.3307 & 0.9508 & -0.0001 & -0.0024 \end{bmatrix}$$

$$F_5 = 1 \times 10^3 \times \begin{bmatrix} 0.0756 & -0.0827 & -0.0929 & -0.2906 & -0.0006 & 0.0001 \\ -0.0541 & -0.0572 & 0.4253 & 0.0378 & 0.0006 & 0.0001 \\ 0.1120 & -0.2132 & -0.1289 & -0.1682 & -0.0006 & 0.0000 \\ 0.1330 & -0.0837 & 0.2471 & 0.0637 & 0.0006 & 0.0000 \\ 0.4552 & 0.1271 & -4.6169 & 4.0438 & -0.0000 & -0.0048 \\ 2.2777 & -2.0084 & -2.2416 & 1.9765 & 0.0010 & -0.0044 \end{bmatrix}$$

$$F_6 = 1 \times 10^3 \times \begin{bmatrix} 0.0997 & -0.8702 & -0.1165 & 0.4844 & -0.0006 & 0.0000 \\ -0.0164 & -0.1821 & 0.3881 & 0.1608 & -0.0006 & 0.0000 \\ 0.1018 & -0.5099 & -0.1189 & 0.1238 & -0.0006 & 0.0000 \\ -0.2711 & -0.1656 & 0.6448 & 0.1443 & -0.0006 & 0.0000 \\ 0.8663 & -8.8729 & -5.0215 & 4.5631 & -0.0020 & -0.0018 \\ -3.3844 & -0.9662 & 3.3307 & 0.9508 & -0.0001 & -0.0024 \end{bmatrix}$$

$$F_7 = 1 \times 10^3 \times \begin{bmatrix} 0.0997 & -0.8702 & -0.1165 & 0.4844 & 0.0006 & 0.0000 \\ -0.0164 & -0.1821 & 0.3881 & 0.1608 & 0.0006 & 0.0000 \\ 0.1018 & -0.5099 & -0.1189 & 0.1238 & 0.0006 & 0.0000 \\ -0.2711 & -0.1656 & 0.6448 & 0.1443 & 0.0006 & 0.0000 \\ -0.8663 & 8.8729 & 5.0215 & -4.5631 & -0.0020 & -0.0018 \\ 3.3844 & 0.9662 & -3.3307 & -0.9508 & -0.0001 & -0.0024 \end{bmatrix}$$

$$F_8 = 1 \times 10^3 \times \begin{bmatrix} 0.0756 & -0.0827 & -0.0929 & -0.2906 & 0.0006 & -0.0001 \\ -0.0541 & -0.0572 & 0.4253 & 0.0378 & -0.0006 & -0.0001 \\ 0.1120 & -0.2132 & -0.1289 & -0.1682 & 0.0006 & 0.0000 \\ 0.1330 & -0.0837 & 0.2471 & 0.0637 & -0.0006 & 0.0000 \\ -0.4552 & -0.1271 & 4.6169 & -4.0438 & 0.0000 & -0.0048 \\ -2.2777 & 2.0084 & 2.2416 & -1.9765 & 0.0010 & -0.0044 \end{bmatrix} \tag{42}$$

$$K_1 = 1 \times 10^3 \times \begin{bmatrix} -0.0002 & -0.0000 & 0.0585 & -0.0067 \\ -0.0000 & -0.0002 & 0.0363 & -0.0063 \\ -0.0002 & -0.0000 & 0.0394 & -0.0126 \\ -0.0000 & -0.0002 & 0.0496 & -0.0297 \\ -0.0013 & 0.0013 & 2.4015 & 2.1286 \\ 0.0000 & -0.0000 & 1.3615 & 2.9284 \end{bmatrix}$$

$$K_2 = 1 \times 10^3 \times \begin{bmatrix} -0.0002 & 0.0000 & 0.0000 & -0.0658 \\ -0.0000 & -0.0002 & 0.0000 & 0.0616 \\ -0.0002 & 0.0000 & 0.0000 & -0.0150 \\ 0.0000 & -0.0002 & 0.0000 & 0.0105 \\ -0.0013 & -0.0013 & 0.0000 & 5.7564 \\ 0.0000 & 0.0000 & 0.0000 & 5.2503 \end{bmatrix}$$

$$K_3 = 1 \times 10^3 \times \begin{bmatrix} -0.0002 & 0.0000 & 0.0000 & 0.0658 \\ -0.0000 & -0.0002 & 0.0000 & -0.0616 \\ -0.0002 & -0.0000 & 0.0000 & 0.0150 \\ 0.0000 & -0.0002 & 0.0000 & -0.0105 \\ 0.0013 & 0.0013 & 0.0000 & 5.7564 \\ 0.0000 & 0.0000 & 0.0000 & 5.2503 \end{bmatrix}$$

$$K_4 = 1 \times 10^3 \times \begin{bmatrix} -0.0002 & 0.0000 & -0.0585 & 0.0067 \\ -0.0000 & -0.0002 & -0.0363 & 0.0063 \\ -0.0002 & -0.0000 & -0.0394 & 0.0126 \\ 0.0000 & -0.0002 & -0.0496 & 0.0297 \\ 0.0013 & -0.0013 & 2.4015 & 2.1286 \\ 0.0000 & 0.0000 & 1.3615 & 2.9284 \end{bmatrix}$$

$$K_5 = 1 \times 10^3 \times \begin{bmatrix} -0.0002 & -0.0000 & 0.0000 & -0.0658 \\ 0.0000 & -0.0002 & 0.0000 & -0.0616 \\ -0.0002 & 0.0000 & 0.0000 & -0.0150 \\ -0.0000 & -0.0002 & 0.0000 & -0.0105 \\ -0.0013 & 0.0013 & 0.0000 & 5.7564 \\ -0.0000 & 0.0000 & 0.0000 & 5.2503 \end{bmatrix}$$

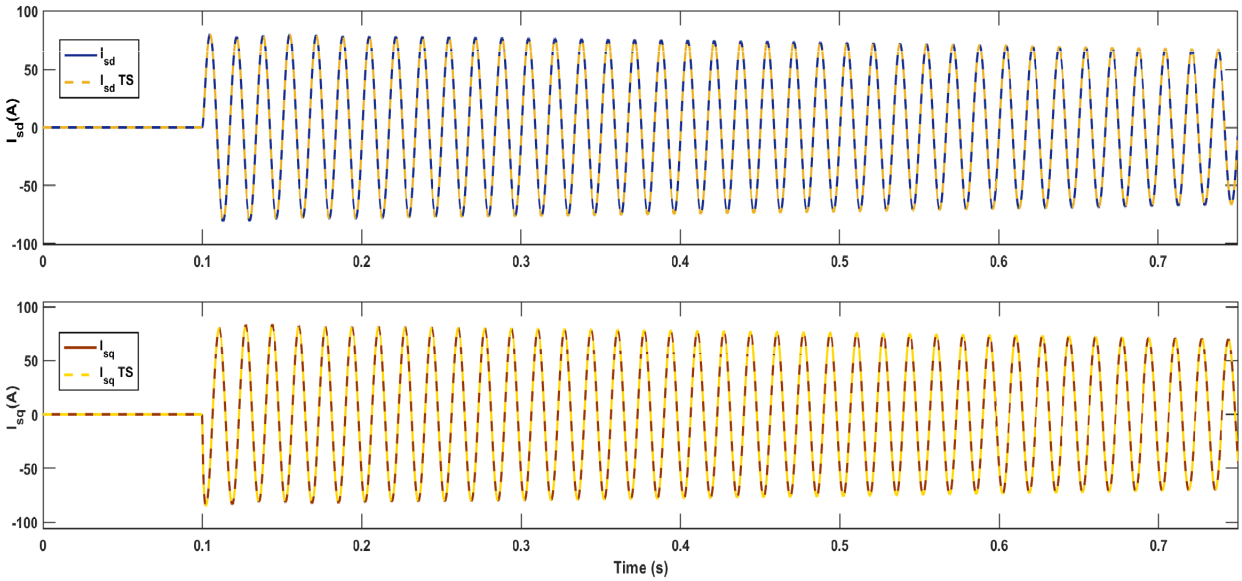

FIGURE 4. I_{sd} and I_{sq} no lineal vs I_{sd} and I_{sq} TS.

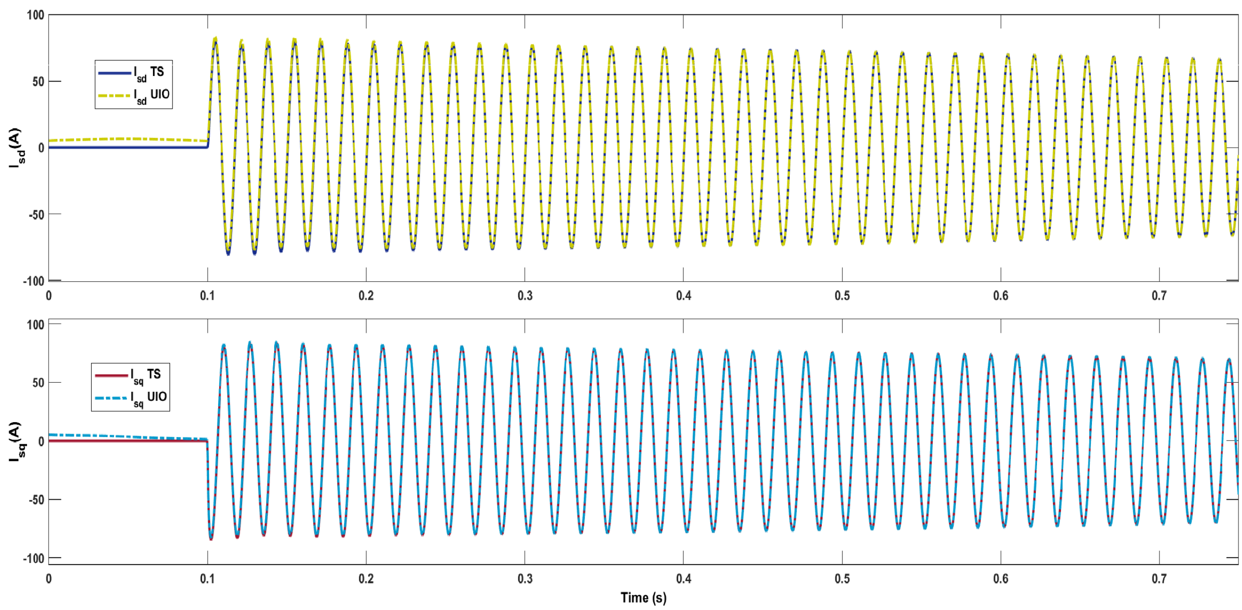

FIGURE 5. I_{sd} and I_{sq} TS vs I_{sd} and I_{sq} TS-UIO.

$$K_6 = 1 \times 10^3 \times \begin{bmatrix} -0.0002 & 0.0000 & 0.0585 & -0.0067 \\ 0.0000 & -0.0002 & -0.0363 & 0.0063 \\ -0.0002 & 0.0000 & 0.0394 & -0.0126 \\ 0.0000 & -0.0002 & -0.0496 & 0.0297 \\ -0.0013 & -0.0013 & 2.4015 & 2.1286 \\ 0.0000 & 0.0000 & 1.3615 & 2.9284 \end{bmatrix}$$

$$K_7 = 1 \times 10^3 \times \begin{bmatrix} -0.0002 & 0.0000 & -0.0585 & 0.0067 \\ 0.0000 & -0.0002 & 0.0363 & -0.0063 \\ -0.0002 & 0.0000 & -0.0394 & 0.0126 \\ 0.0000 & -0.0002 & 0.0496 & -0.0297 \\ 0.0013 & 0.0013 & 2.4015 & 2.1286 \\ -0.0000 & 0.0000 & 1.3615 & 2.9284 \end{bmatrix}$$

$$K_8 = 1 \times 10^3 \times \begin{bmatrix} -0.0002 & 0.0000 & 0.0000 & 0.0658 \\ 0.0000 & -0.0002 & 0.0000 & 0.0616 \\ -0.0002 & 0.0000 & 0.0000 & 0.0150 \\ 0.0000 & -0.0002 & 0.0000 & 0.0105 \\ 0.0013 & -0.0013 & 0.0000 & 5.7564 \\ 0.0000 & 0.0000 & 0.0000 & 5.2503 \end{bmatrix} \quad (43)$$

$$T_{1-8} = \begin{bmatrix} 0.4920 & 0 & 0.4999 & 0 & 0 & 0 \\ 0 & 0.4920 & 0 & 0.4999 & 0 & 0 \\ 0.4999 & 0 & 0.5080 & 0 & 0 & 0 \\ 0 & 0.4999 & 0 & 0.5080 & 0 & 0 \\ 0 & 0 & 0 & 0 & 1 & 0 \\ 0 & 0 & 0 & 0 & 0 & 1 \end{bmatrix} \quad (44)$$

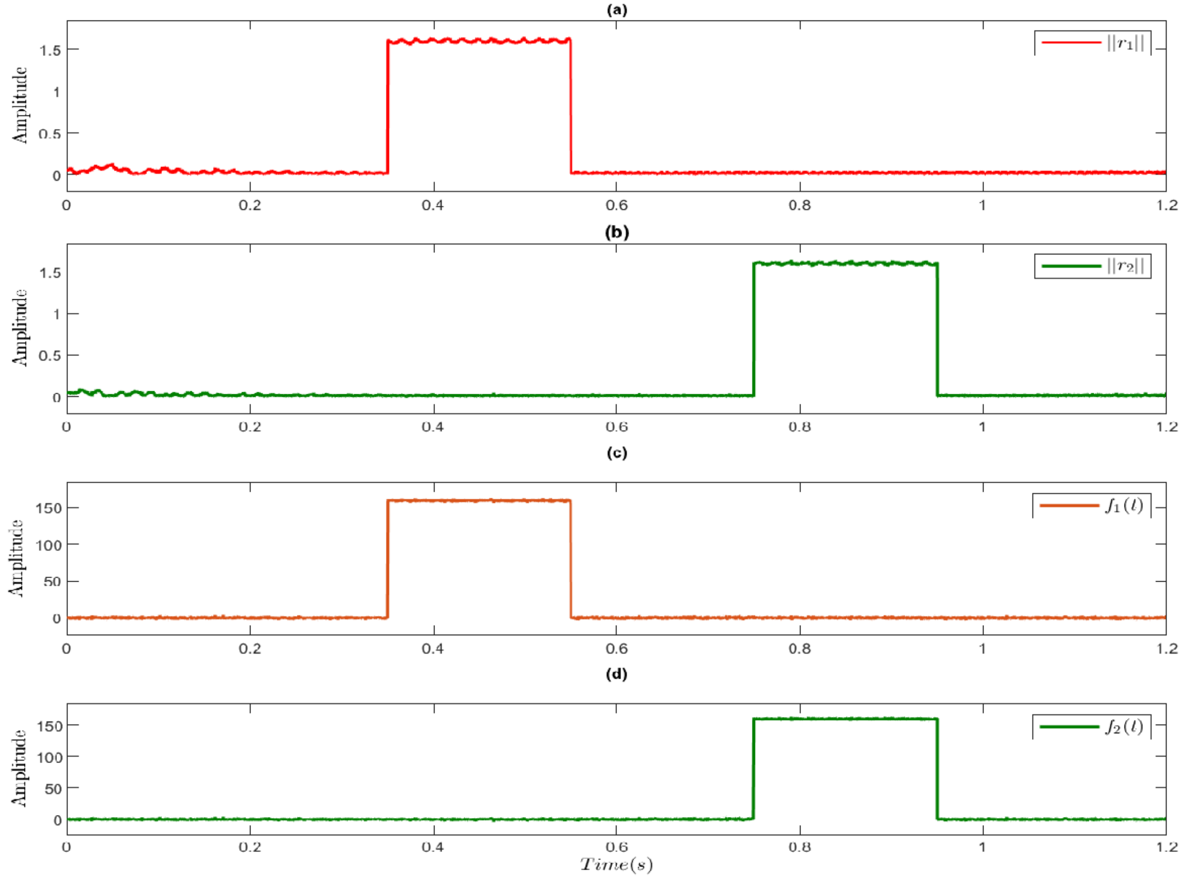

FIGURE 6. Normalised residuals $\|r_1(t)\|$, $\|r_2(t)\|$, $f_1(t)$, $f_2(t)$ are induced fault signals.

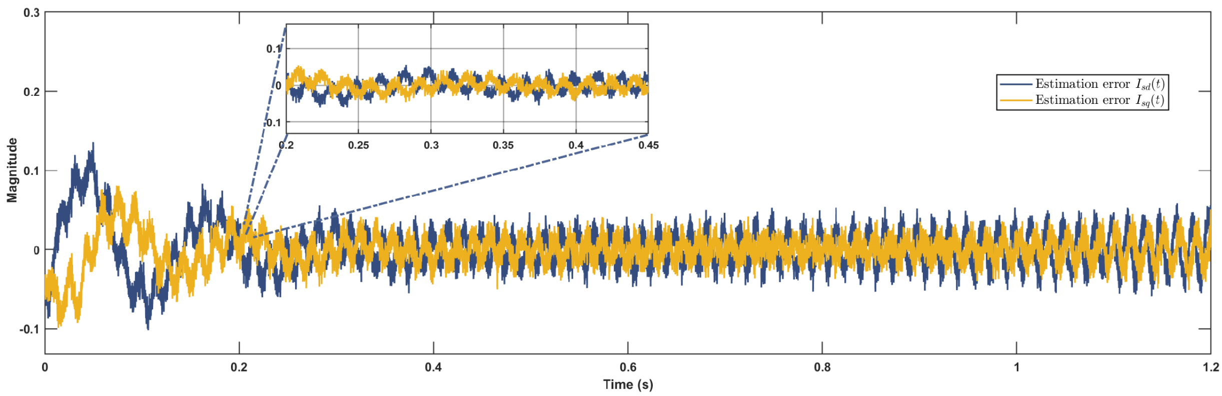

FIGURE 7. Error $e(t)$ between the observer (TS-UIO) and the Takagi-Sugeno (TS) model.

$$H_{1-8} = 1 \times 10^{-3} \times \begin{bmatrix} 0.3153 & 0 & 0 & 0 \\ 0 & 0.3153 & 0 & 0 \\ -0.3103 & 0 & 0 & 0 \\ 0 & -0.3103 & 0 & 0 \\ 0 & 0 & 0.8333 & 0 \\ 0 & 0 & 0 & 0.8333 \end{bmatrix} \quad (45)$$

VI. FAULT DIAGNOSIS

Fault detection in the sensor in the DOS-like observer bank scheme [27] (Figure 9) generates a vector $|r_n(t)|$ representing the normalised residual of the n-th observer. Its n-th component uses all inputs and only the n-th output [8].

$$\|r_n(t)\| = \|y_n(t) - C_n\hat{x}_n(t)\| \quad (46)$$

The set of residuals is used to distinguish between one fault and another, i.e., fault is isolated using a set of residuals as shown in the table 2.

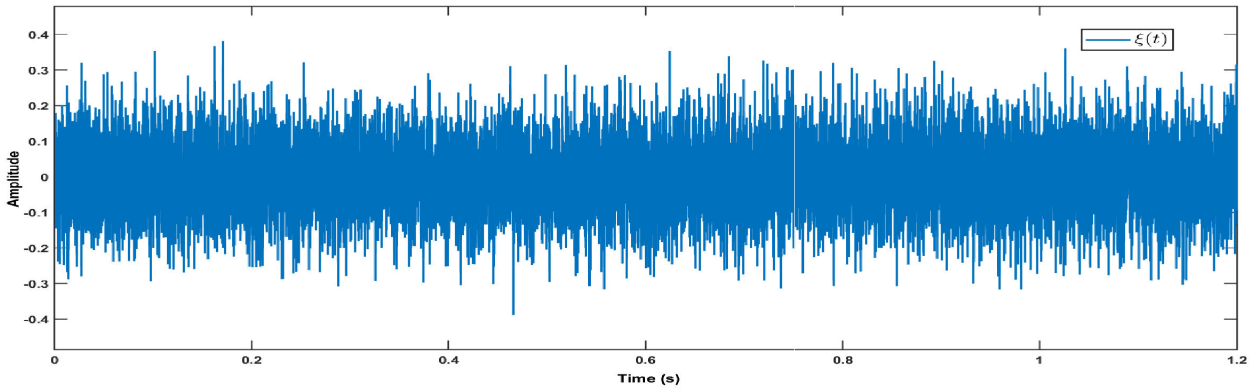

FIGURE 8. Disturbance $\xi(t)$.

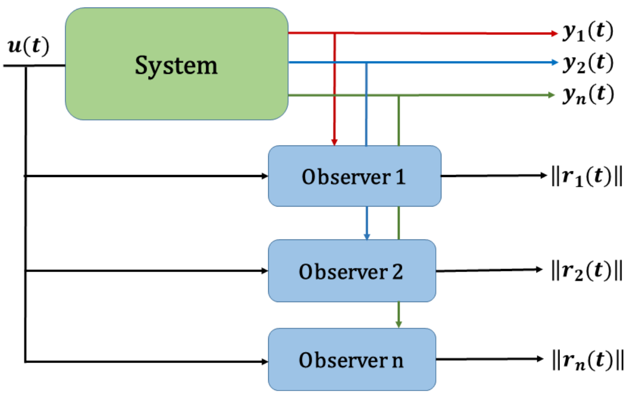

FIGURE 9. Two-bank observers scheme for detecting faults in sensors.

TABLE 2. Incidence Matrix for the Two Schemes for Sensor Fault Isolation.

Fault	f_1	f_2	$\cdots$	f_n
$\|r_1(t)\|$	1	0	$\cdots$	0
$\|r_2(t)\|$	0	1	$\cdots$	0
$\vdots$	$\vdots$	$\vdots$	$\ddots$	$\vdots$
$\|r_n(t)\|$	0	0	$\cdots$	1

VII. DISCUSSIONS

To demonstrate the application of the proposed method, we consider the measurement noise in the sensors I_{sd} and $I_s q$ with a power of $1 \times 10^{-6}W$ and the uncertainty given in the unknown input of the system $\xi(t)$ can be shown in Figure 8. Two known inputs, $u_1(t) = 220sin(377t)$ and $u_2(t) = 220sin(377t - \frac{2*pi}{3})$ for all t are also considered. For the simulation, the initial conditions $x(0) = \left[0.2\ 0.2\ 0.2\ 0.2\ 0\ 0\right]^T$ of the observer and $x(0) = \left[0\ 0\ 0\ 0\ 0\ 0\right]^T$ for the Takagi-Sugeno system were considered, as shown in Figure 5, to demonstrate the convergence of the TS-UIO observer with the non-linear system of the pitch system under study.

In the Figure 6 showing Fault Diagnostics (FDI) scheme [28], the fault is induced in the stator current sensor d (sensor 1), indicated as $f_1(t)$, and a fault is induced in the stator current sensor q (sensor 2), indicated as $f_2(t)$, Both faults can be shown in Figure 6 (c) and (d). This failure can be described as a ramp or step function to represent slow or abrupt failures. Abrupt failures are considered in this paper. It's also important to note that sensor failures are modeled as additive bias, i.e., they can be described as calibration or compensation problems. The signals of the normalised residuals are shown in Figure 6 and Figure 6 (a) and (b) [29]. Under fault-free conditions, the TS-UIO observer [30] can estimate the states despite measurement noise in the sensor and uncertainty due to the action of the wind force. The purpose of sensor fault detection is fulfilled by the fault diagnosis scheme (FDI) [31]; the proposed unknown input observer (UIO) has the robustness to detect faults in the presence of uncertainty in one of the states and measurement noise. Finally, Figure 7, shows the error between the observer (TS-UIO) and the Takagi-Sugeno (TS) model; for the states I_{sd} vs $I_{sd}TS$ and I_{sq} vs $I_{sq}TS$.

VIII. CONCLUSION

This paper shows the design of TS-UIO applied to fault diagnosis in an active electrical pitch system. It is important to mention that in this work, the Takagi-Sugeno model was used for the system as well as for the observers. The fault diagnosis algorithm was tested in simulation, and according to the results, we may assume that the TS-UIO is a good tool for resolving the model-based fault diagnosis problem. The Takagi-Sugeno Unknown Inputs observers allow the sensor fault detection for the systems, in this case, study the pitch system of a wind turbine.

This work considers the variable parameter conditions denoted by the nonlinearities $x_3(t) \in [-0.4, 0.4]$ (Wb), $x_4(t) \in [-0.4, 0.4]$ (Wb) and $w(t) \in [-378, 378]$ rad/s and the analysis of the wind maps provided by the National Renewable Energy Laboratory (NREL) in the user manual [32], cites the maximum torque supported by the wind turbine blades, for this reason it is possible to measure the unknown input to the system.

The comparison with [33], the nonlinear system, shows that the observer proposed in this work is a robust observer of disturbances, even when there is measurement noise, the proposed scheme is able to observe the behaviour of the states. Another important consideration in the work is considering two simultaneous faults during simulation time at different times [33] as can be seen in Figure 6.

An additional contribution of the proposed work is the evaluation of the stress to which the wind turbine blades are subjected, considering this stress as an unknown input because it depends on the wind and weather conditions where the wind turbine is installed. It is important to mention in future work: propose a method of the diagnosis of faults in the pitch actuator proposed with an observer of unknown inputs (UIO) and add delay times in the measurements to verify the robustness of the observer of unknown inputs (UIO), being this observer one of the most studied by the scientific community.

Finally, it can be concluded that there is an increasing demand for renewable wind or solar energy in various sectors, including industry, companies, homes, buildings, and electric car charging. It is crucial to ensure the quality of this energy to prevent any harm to equipment or systems that run on it.

ACKNOWLEDGMENT

Acknowledgment is given to TecNM, Campus Tuxtla, for providing the facilities necessary for the development of this work as part of the Doctorate in Engineering Sciences. Thanks are also due to Dr. Hector Ricardo Hernández de León and the other academics for their valuable comments and to Dr. Alejandro Medina Santiago for his support.

REFERENCES

[1] J. F. Manwell, J. G. McGowan, and A. L. Rogers, *Wind Energy Explained: Theory, Design and Application*. Hoboken, NJ, USA: Wiley, 2010.

[2] P. F. Odgaard, J. Stoustrup, and M. Kinnaert, "Fault-tolerant control of wind turbines: A benchmark model," *IEEE Trans. Control Syst. Technol.*, vol. 21, no. 4, pp. 1168–1182, Jul. 2013.

[3] D. Wood, *Small Wind Turbines: Analysis, Design, and Application* (Green Energy and Technology Series), 1st ed. London, U.K.: Springer, Nov. 2013, p. 272, doi: 10.1007/978-1-84996-175-2.

[4] W. H. A. Lio, "Blade-pitch control for wind turbine load reductions," M.S. thesis, Dept. Wind Energy, Univ. Sheffield, Sheffield, U.K., 2018. [Online]. Available: https://doi.org/10.1007/978-3-319-75532-8

[5] T. Burton, D. Sharpe, N. Jenkins, and E. Bossanyi, *Wind Energy Handbook*, vol. 2. Hoboken, NJ, USA: Wiley, 2001.

[6] N. Singh, B. Pratap, and A. Swarup, "Nonlinear robust observer based adaptive control design for variable speed wind turbine," *J. Eng. Res.*, vol. 7, no. 3, pp. 258–285, Sep. 2019.

[7] Z. Khaouch, M. Zekraoui, J. Bengourram, N. Kouider, and M. Mabrouki, "Mechatronic modeling of a 750 kW fixed-speed wind energy conversion system using the bond graph approach," *ISA Trans.*, vol. 65, pp. 418–436, Nov. 2016.

[8] J. Chen and R. J. Patton, *Robust Model-Based Fault Diagnosis for Dynamic Systems* (The International Series on Asian Studies in Computer and Information Science), 1st ed. New York, NY, USA: Springer, Nov. 2012, p. 375. [Online]. Available: https://doi.org/10.1007/978-1-4615-5149-2

[9] S. Gómez-Peñate, G. Valencia-Palomo, F. López-Estrada, C. Astorga-Zaragoza, R. A. Osornio-Rios, and I. Santos-Ruiz, "Sensor fault diagnosis based on a sliding mode and unknown input observer for Takagi–Sugeno systems with uncertain premise variables," *Asian J. Control*, vol. 21, no. 1, pp. 339–353, Jan. 2019.

[10] M. Witczak, "Fault diagnosis and fault-tolerant control strategies for non-linear systems," in *Analytical and Soft Computing Approaches* (Lecture Notes in Electrical Engineering), 1st ed. Switzerland: Springer, Aug. 2016, p. 229. [Online]. Available: https://doi.org/10.1007/978-3-319-03014-2

[11] C. L. Bottasso, F. Campagnolo, and V. Petrović, "Wind tunnel testing of scaled wind turbine models: Beyond aerodynamics," *J. Wind Eng. Ind. Aerodynamics*, vol. 127, pp. 11–28, Apr. 2014.

[12] F. P. G. Márquez, A. M. Tobias, J. M. P. Pérez, and M. Papaelias, "Condition monitoring of wind turbines: Techniques and methods," *Renew. Energy*, vol. 46, pp. 169–178, Oct. 2012.

[13] Z. Gao, S. X. Ding, and C. Cecati, "Real-time fault diagnosis and fault-tolerant control," *IEEE Trans. Ind. Electron.*, vol. 62, no. 6, pp. 3752–3756, Jun. 2015.

[14] X. Yin, W. Zhang, Z. Jiang, and L. Pan, "Adaptive robust integral sliding mode pitch angle control of an electro-hydraulic servo pitch system for wind turbine," *Mech. Syst. Signal Process.*, vol. 133, Nov. 2019, Art. no. 105704.

[15] P. H. S. Coutinho, R. F. Araújo, A.-T. Nguyen, and R. M. Palhares, "A multiple-parameterization approach for local stabilization of constrained Takagi–Sugeno fuzzy systems with nonlinear consequents," *Inf. Sci.*, vol. 506, pp. 295–307, Jan. 2020.

[16] K. Tanaka and H. O. Wang, *Fuzzy Control Systems Design and Analysis*. Hoboken, NJ, USA: Wiley, 2001.

[17] T. M. Guerra, R. Márquez, A. Kruszewski, and M. Bernal, "$H\infty$ LMI-based observer design for nonlinear systems via Takagi–Sugeno models with unmeasured premise variables," *IEEE Trans. Fuzzy Syst.*, vol. 26, no. 3, pp. 1498–1509, Jun. 2018.

[18] D. Rotondo, V. Puig, and F. Nejjari, "On the analogies in control design of non-linear systems using LPV and Takagi–Sugeno models," in *Proc. 5th Int. Conf. Syst. Control (ICSC)*, May 2016, pp. 225–230.

[19] J. A. Guzmán-Rabasa, F. R. López-Estrada, B. M. González-Contreras, G. Valencia-Palomo, M. Chadli, and M. Pérez-Patricio, "Actuator fault detection and isolation on a quadrotor unmanned aerial vehicle modeled as a linear parameter-varying system," *Meas. Control*, vol. 52, nos. 9–10, pp. 1228–1239, Nov. 2019.

[20] J. M. Palma, C. F. Morais, and R. C. L. F. Oliveira, "\mathscr$H_2$ gain-scheduled filtering for discrete-time LPV systems using estimated time-varying parameters," in *Proc. Annu. Amer. Control Conf. (ACC)*, Jun. 2018, pp. 4367–4372.

[21] A.-T. Nguyen, T. Q. Dinh, T.-M. Guerra, and J. Pan, "Takagi–Sugeno fuzzy unknown input observers to estimate nonlinear dynamics of autonomous ground vehicles: Theory and real-time verification," *IEEE/ASME Trans. Mechatronics*, vol. 26, no. 3, pp. 1328–1338, Jun. 2021.

[22] D. Zhao, H. Keung Lam, Y. Li, S. X. Ding, and S. Liu, "A novel approach to state and unknown input estimation for Takagi–Sugeno fuzzy models with applications to fault detection," *IEEE Trans. Circuits Syst. I, Reg. Papers*, vol. 67, no. 6, pp. 2053–2063, Jun. 2020.

[23] M. Mousavi, A. Mostafavi, M. Moradi, A. Chaibakhsh, M. Kordestani, M. Derakhshanfar, and M. Saif, "Robust fault isolation of gas turbines via nonlinear intelligent observer and Takagi–Sugeno fuzzy inference system," *IEEE Sensors J.*, vol. 23, no. 20, pp. 25075–25085, 2023.

[24] B. Marx, D. Ichalal, J. Ragot, D. Maquin, and S. Mammar, "Unknown input observer for LPV systems," *Automatica*, vol. 100, pp. 67–74, Feb. 2019.

[25] F. Xu, J. Tan, X. Wang, V. Puig, B. Liang, B. Yuan, and H. Liu, "Generalized set-theoretic unknown input observer for LPV systems with application to state estimation and robust fault detection," *Int. J. Robust Nonlinear Control*, vol. 27, no. 17, pp. 3812–3832, Nov. 2017.

[26] B. Chen, P. C. Matthews, and P. J. Tavner, "Automated on-line fault prognosis for wind turbine pitch systems using supervisory control and data acquisition," *IET Renew. Power Gener.*, vol. 9, no. 5, pp. 503–513, Jul. 2015.

[27] M. Zhou, Z. Wang, and Y. Shen, "Fault detection and isolation method based on H-/H_∞ unknown input observer design in finite frequency domain," *Asian J. Control*, vol. 19, no. 5, pp. 1777–1790, Sep. 2017.

[28] T. Youssef, M. Chadli, H. R. Karimi, and R. Wang, "Actuator and sensor faults estimation based on proportional integral observer for TS fuzzy model," *J. Franklin Inst.*, vol. 354, no. 6, pp. 2524–2542, Apr. 2017.

[29] A. Mokhtari and M. Belkhiri, "An adapative observer based FDI for wind turbine benchmark model," in *Proc. 8th Int. Conf. Model., Identificat. Control (ICMIC)*, Nov. 2016, pp. 742–746.

[30] H. H. Alhelou, M. E. H. Golshan, and J. Askari-Marnani, ''Robust sensor fault detection and isolation scheme for interconnected smart power systems in presence of RER and EVs using unknown input observer,'' *Int. J. Electr. Power Energy Syst.*, vol. 99, pp. 682–694, Jul. 2018.

[31] F. R. López-Estrada, D. Theilliol, C. M. Astorga-Zaragoza, J. C. Ponsart, G. Valencia-Palomo, and J. Camas-Anzueto, ''Fault diagnosis observer for descriptor Takagi–Sugeno systems,'' *Neurocomputing*, vol. 331, pp. 10–17, Feb. 2019. [Online]. Available: https://www.sciencedirect.com/science/article/pii/S0925231218313997

[32] J. M. Jonkman and M. L. Buhl, ''FAST user's guide,'' Nat. Renew. Energy Lab., Golden, CO, USA, Tech. Rep. NREL/TP-500-38230, 2005, vol. 365, p. 366.

[33] V. Borja-Jaimes, M. Adam-Medina, B. Y. López-Zapata, L. G. V. Valdés, L. Claudio Pachecano, and E. M. S. Coronado, ''Sliding mode observer-based fault detection and isolation approach for a wind turbine benchmark,'' *Processes*, vol. 10, no. 1, p. 54, Dec. 2021. [Online]. Available: https://www.mdpi.com/2227-9717/10/1/54

JORGE IVÁN BERMÚDEZ RODRÍGUEZ received the M.Sc. degree from the Universidad de Ciencia y Tecnología Descartes, in 2014. He is currently pursuing the Ph.D. degree in engineering sciences with the Department of Electronic Engineering, Tecnológico Nacional de México/Instituto Tecnológico de Tuxtla Gutiérrez (ITTG). His research interest includes fault diagnosis algorithms designed for nonlinear systems using Takagi-Sugeno modeling.

HÉCTOR RICARDO HERNÁNDEZ-DE-LEÓN (Senior Member, IEEE) was born in Tuxtla, Chiapas, in 1959. He received the B.S. degree in electronic engineering from the National Polytechnic Institute of Mexico City, in 1982, and the M.S. and Ph.D. degrees in automatic systems from the National Institute of Applied Sciences, INSA Toulouse, France, in 2006. He is currently a full-time Professor and a Researcher with the Department of Electrical and Electronics Engineering, Instituto Tecnológico de Tuxtla Gutiérrez (ITTG), Chiapas, Mexico. He is integrated into the research group ''process automation'' of M.S. and Ph.D. programs in mechatronics engineering with ITTG. His research interests include supervisory control, diagnosis of complex processes, automatic control applied to industrial processes, communications technologies, energy harvesting, and the IoT. Some of the current works are intelligent control and diagnosis of potable water plants and biodiesel diagnosis and prognosis.

JUAN ANZUREZ MARÍN received the B.E. degree in electrical engineering from Universidad Michoacana de San Nicolás de Hidalgo (UMSNH), Morelia, Mexico, in 1991, the M.Sc. degree in electronic engineering from Instituto Tecnologico de Chihuahua, Mexico, in 1997, and the Ph.D. degree in electrical engineering option automatic control from Centro de Investigacion y Estudios Avanzados del IPN (CINVESTAV), Guadalajara Campus, Mexico, in 2007. Since 1987, he has been an Associate Professor with the Department of Electrical Engineering, UMSNH. His research interests include instrumentation and control systems and fault diagnosis algorithms designed for nonlinear systems using Takagi-Sugeno modeling.

ALEJANDRO MEDINA SANTIAGO graduated in electronics engineer from TecNM Campus, Tuxtla, in 2000, and the Master of Science and Doctor of Science degrees in electrical engineering from the Centre for Research and Advanced Studies of the National Polytechnic Institute, in 2002 and 2008, respectively. He was an Electronics Engineer with the Technological Institute of Tuxtla Gutierrez. Currently, he is a Researcher with the Department of Computer Science, Institute National for Astrophysics, Optics and Electronics. He is also the Founder and the Sub-Director of the Centre for Research, Development and Technological Innovation, University of Science and Technology Descartes UNAM. His research interests include signal processing, cybersecurity, the IoT, Industry 4.0, VLSI integrated circuit design, and intelligent systems design using deep learning, neural networks, and fuzzy logic.

ELÍAS NEFTALÍ ESCOBAR GÓMEZ (Member, IEEE) was born in Tuxtla, Chiapas, in 1971. He received the B.S. degree in industrial engineering from Instituto Tecnológico de Tuxtla Gutiérrez (ITTG), in 1993, the M.S. degree from the Orizaba Institute of Technology, in 2000, and the Ph.D. degree from CIDESI, in 2009. He is currently a full-time Professor and a Researcher with ITTG. He is integrated into the research group ''Process Automation'' of M.S. and Ph.D. programs in mechatronics engineering with ITTG. His research interests include intelligent control applied to industrial processes and Industry 4.0. He is a Senior Member of IISE.

BETTY YOLANDA LÓPEZ ZAPATA received the Doctor of Science degree in electronic engineering from Centro Nacional de Investigación y Desarrollo Tecnológico. She is currently a Research Professor with Universidad Politécnica de Chiapas. She has different articles published in magazines and conferences referring to automation, control, renewable energies, fault diagnosis, and fault-tolerant control. Her research interests include line of investigation control, fault diagnosis, and state observers. She is a member of the National System of Researchers (SNI), the Information Security Investigation Commission, and the Information Security Culture Promotion Commission.

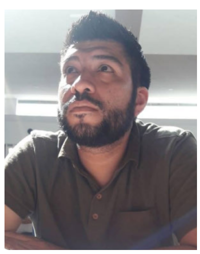

JULIO ALBERTO GUZMÁN-RABASA received the M.Sc. degree from Instituto Tecnológico de Tuxtla Gutiérrez (ITTG), in 2017, and the Ph.D. degree in engineering sciences from the Department of Electronic Engineering, Tecnológico Nacional de México/ITTG, in 2021. His research interests include centered on fault diagnosis, fault-tolerant control systems, Takagi-Sugeno systems, LPV systems, and their applications.